Energy-Efficient Data Collection and Resource Allocation in Age-Aware IoV

Fangzhe Chen [1], Minghui Liwang [2], Zhibin Gao [2], and Lianfen Huang [2]

[1]Department of Information and Communication Engineering and the Key Laboratory of Digital Fujian on IoT Communication
[2]Affiliation not available

July 29, 2022

Abstract

The emergence of Internet of Vehicles (IoV) has facilitated many attractive vehicular applications that require massive sensed data and timely data analysis. Data collection and resource allocation are critical issues in IoV for timely data processing in dynamic network environments. However, the energy consumption of IoV infrastructure and vehicles pose challenges to developing sustainable vehicular communication and networking infrastructure. Moreover, the communication and computing resources are generally insufficient to support the transmission and analysis of the excessive data. Vehicular data are often updated periodically, which makes much of which outdated, or useless for vehicular applications, and thus leads to large latency and tremendous energy consumption. To this end, age of Information (AoI) has been introduced as a novel metric to characterize data freshness. Satisfying the state update AoI constraint is of great significance to guarantee the freshness of the IoV system. In this paper, we design a sampling strategy with responsive transmission and computing (e.g., no waiting latency), and investigate an energy minimization problem under peak AoI constraints in age-aware vehicular networks. We decouple the problem as a minimum set cover problem, and a convex problem, and propose a joint sampling selection and resource allocation (JSRA) algorithm to obtain the approximate optimal solution. We evaluate the proposed sampling selection and resource allocation strategy and JSRA algorithm by experiments on the simulation of urban mobilty (SUMO). Numerical results show that the proposed sampling strategy and algorithm outperform existing methods in terms of energy consumption, especially for the scenario with dense vehicles and pedestrians.

Energy-Efficient Data Collection and Resource Allocation in Age-Aware IoV

Fangzhe Chen, Minghui Liwang, *Member, IEEE,* Zhibin Gao*, *Member, IEEE,* Lianfen Huang

Abstract—The emergence of Internet of Vehicles (IoV) has facilitated many attractive vehicular applications that require massive sensed data and timely data analysis. Data collection and resource allocation are critical issues in IoV for timely data processing in dynamic network environments. However, the energy consumption of IoV infrastructure and vehicles pose challenges to developing sustainable vehicular communication and networking infrastructure. Moreover, the communication and computing resources are generally insufficient to support the transmission and analysis of the excessive data. Vehicular data are often updated periodically, which makes much of which outdated, or useless for vehicular applications, and thus leads to large latency and tremendous energy consumption. To this end, age of Information (AoI) has been introduced as a novel metric to characterize data freshness. Satisfying the state update AoI constraint is of great significance to guarantee the freshness of the IoV system. In this paper, we design a sampling strategy with responsive transmission and computing (e.g., no waiting latency), and investigate an energy minimization problem under peak AoI constraints in age-aware vehicular networks. We decouple the problem as a minimum set cover problem, and a convex problem, and propose a joint sampling selection and resource allocation (JSRA) algorithm to obtain the approximate optimal solution. We evaluate the proposed sampling selection and resource allocation strategy and JSRA algorithm by experiments on the simulation of urban mobilty (SUMO). Numerical results show that the proposed sampling strategy and algorithm outperform existing methods in terms of energy consumption, especially for the scenario with dense vehicles and pedestrians.

Index Terms—Internet of Vehicles, energy consumption, peak AoI, data collection, resource allocation.

I. INTRODUCTION

WITH the advancement of mobile communications, Internet of Vehicles (IoV) and artificial intelligence technology, a large number of vehicular applications have been emerged, such as real-time situational awareness [1], virtual reality [2], digital twin [3] and autonomous driving [4]. To satisfy the performance requirements of vehicular applications, vehicles will be equipped with diverse types of sensors (e.g., tachographs, lateral acceleration sensors, GPS, Cameras, Lidar, etc.). With the evolution of vehicle-to-everything (V2X) communications, vehicles with communication and sensing capa-

The authors are with the Department of Information and Communication Engineering and the Key Laboratory of Digital Fujian on IoT Communication, Architecture and Security Technology, Xiamen University, Xiamen 361005, China (e-mail: chenfangzhe@stu.xmu.edu.cn; lfhuang@xmu.edu.cn; gaozhibin@xmu.edu.cn; minghuilw@xmu.edu.cn).

bilities can be considered as mobile sensors that continuously sense informative status updates about their surroundings, providing public service for IoV. Limited by constrained sensing coverage, vehicles collect surrounding sensed data in the sensing subdomain and transmit sensed data to the control center by vehicle-to-infrastructure (V2I) communication [5]. Then, the control center aggregates and analyzes sensed data to serve vehicular applications such as traffic management, digital twin, etc.

Vehicular applications generally require vehicles to generate a huge amount of sensed data. How to efficiently collect and process massive amounts of data from hundreds of moving vehicles is challenging for IoV infrastructure. First, the sampling frequency of the data exceeds the requirements of the application in most cases, making data redundant. Then, the sensing scopes of the vehicles have overlapping parts. For a vehicular application, much of the sensed data is duplicated. Finally, the sheer amount of redundant data may exhaust transmission and computing resources, resulting in heavy overhead [6]. To address the above challenges, avoiding unnecessary data collection and allocating resources appropriately to transmit and process data is critical.

Due to the high dynamics of the IoV, the timeliness of data collection is of great significance. The traditional metric based on delay can only reflect the transmission and computing time of data, which, however, cannot express the update frequency. [7] proposed the concept of Age of Information (AoI) to quantify the freshness of sensed data. AoI is defined as the elapsed time since the last received state information update data was generated, which has been extensively researched in various fields such as queuing models [8], [9], energy harvesting [10], and data forwarding [6]. However, these work focus on minimizing the average AoI. Average AoI can not reflect the extreme AoI events with low probability, which are fatal in the IoV. Moreover, the cost of electricity from the IoV infrastructure and the fuel emissions from vehicles will place an increasing energy burden on the IoV system [11]. The collection and analysis of massive data will consume large quantities energy in the IoV infrastructure, making the development of sustainable vehicle communication and network infrastructure critical. Most of the existing energy saving researches consider delay constraints [12], [13]. Under AoI constraints, how to adaptively collect data and manage resources to minimize energy consumption is a fundamental but challenging problem. This motivates the current work.

In this paper, we propose a energy-efficient sampling selection and resource allocation strategy. Specifically, we use a directed graph to represent the connectivity among roads,

with each node representing a road segment. To evaluate the freshness of data, we establish a weighted AoI model by integrating the density of vehicles and pedestrians. Moreover, a no-wait sampling slot model and a optimal sampling selection and resource allocation is proposed which reduce energy consumption under AoI constraints. Based on which, an energy consumption minimization problem is formulated which jointly considers node selection and resource allocation. Since it is complicated to solve the problem directly, we decouple the problem as a minimum set cover problem and a convex problem, and propose a joint sampling selection and resource allocation (JSRA) algorithm to obtain the approximate solution. Contributions of our paper are summarized as follows.

- We model the correlations between sampled data as directed graphs and propose a weighted AoI model to measure data quality.
- we a propose joint sampling and resource allocation strategy, and consider the energy minimization problem under AoI constraints. On this basis, we design a sampling time slot to ensure sufficient transmission and computing resources in sampling slot to reduce the peak weighted AoI of data.
- We decouple the energy minimization problem into a minimum set covering problem as well as a convex optimization problem, and propose the joint selection and resource allocation (JSRA) algorithm to obtain an approximate solution.
- We conduct experiments based on real-world vehicle trajectories on the simluation of urban mobility (SUMO) platform. Simulation results demonstrate the better performance of the proposed scheme compared to the existing methods.

The rest of this paper is organized as follows. In Section II, we review some related works on AoI optimization and energy-efficent in vehicular networks. In Section III, we detail the system model. The peak weight AoI constraints and the energy minimization problem are presented. We analyze the proposed problem and proposed JSRA alorithm to solve it. In Section V, we show the numerical results and evaluate the performance of our scheme and algorithm. The conclusions of our work are presented in Section VI.

II. Related Work

AoI is a metric to characterize the freshness of data and has recently attracted attention from academia. Recently, there has been a lot of work focusing on AoI minimization in the IoV [14]–[20]. To be specific, Li *et al.* [14] proposed a mathematical framework for analyzing vehicle social network age and considered joint optimization of information update rate and transmission probability. Qin *et al.* [16] designed a distributed data collection strategy to address the sensing data sampling of the source vehicle and the data forwarding problem in vehicular sensing networks. The above work focuse on the minimization of average AoI. However, the average AoI cannot reflect extreme AoI events because of the low probability of them. A few works [21]–[23] demonstrate that it is more meaningful to focus on limiting the violation probability of AoI than to average or peak AoI. In [23], Hu *et al.* described the IoT network as a queuing model of M/M/1 and M/D/1 and derived closed expressions for the peak AoI distribution and AoI constraint violation probability. In [24], Abdel-Aziz *et al.* They considered the AoI constraint and studied the transmit power minimization problem. They solved the proposed problem using extreme value theory and Lyapunov optimization techniques. Considering data collection and resource allocation under AoI constraints in vehicular networks is a problem of concern.

Energy-efficiency represents a key issue in IoV. The large number of devices and the communication and computing requirements of IoV applications will lead to a surge in energy consumption in future IoV scenarios. Several works have investigated resource allocation considering energy consumption in the IoV and considered the trade off between energy consumption and delay. Ke *et al.* [25] established a novel computation offloading model and proposed an deep reinforcement learning method that considers both energy and data transmission latency. Yadav *et al.* [26] designed a three-stage computation offloading and resource allocation strategy that jointly considers energy consumption and latency. Zhan *et al.* [27] studied a computational offloading scheduling problem considering scheduling location and scheduling time to reduce latency and energy. Futhermore, some works studied the energy consumption under various constraints. Shang *et al.* [28] investigated a computation offloading strategy and designed a deep learning-based algorithm to minimize energy consumption under multiple constraints. Dong *et al.* [13] proposed an energy-efficient method for task scheduling in vehicular networks based on deep reinforcement learning to optimize the total energy of MEC servers under task delay constraints. However, few of aforementioned work consider the constraints of AoI, since the timeliness of data is critical to the IoV. In this work, we focus on the energy minimization under AoI constraints.

III. System Model

This paper considers the traffic management application, which needs to collect and process traffic data periodliy. As shown in Fig. 1, service devices will be installed on the roadside to manage traffic. We divide management road into N segments, denoted as a set $\mathcal{N} = \{1, 2, ..., N\}$. Each service device integrates an RSU and a computing device. Each road segment will install some sensors to periodically scan for vehicles and pedestrians and estimate their density in each segment. We assume that all vehicles on the road segments of $\mathcal{N}$ are within the communication range of the RSU. At each sampling time slot, the RSU collects traffic data of some vehicles and transmits the data to the computing device for processing and analysis.

A. Directed Graph and Weighted AoI Model

We construct the directed graph $\mathcal{G}(\mathcal{N}, \mathcal{C}, \mathcal{E})$ to establish the relationship between different road segments, where road segments of $\mathcal{N}$ are nodes. $\mathcal{E} = \{\eta_{n,m} : n \in \mathcal{N}, m \in \mathcal{N}\}$ denotes

TABLE I
NOTATIONS AND DEFINITIONS

Notations	Definitions
$n, \mathcal{N}$	road segment node index, set
$m, \mathcal{M}$	sampling node index, set
k	sampling time slot
x_n	a binary varible to indicate whether to sample data at node n
$\eta_{n,m}$	a binary variable to indicate whether node n and node m are connected and adjacent
$z_{m,n}$	a binary varibale to indicate whether the weighted AoI of node n is updated by the sampling of node m
ε_n	the traffic complexity of node n
$\varphi_{n,m}$	the path length from node m to node n
b_n	the sampling data size of node n
P_n	the transmission power of sampling vehicle at node n
G_n	the channel gain between sampling vehicle and service device at node n
B	the total bandwidth
σ^2	the background noise
ξ	the conversion coefficient between computing complexity and traffic complexity
γ_n	the proportion of bandwidth allocation
f_n	the computing rate for processing node n
κ	the effective capacitance coefficient
$a_n(t)$	the AoI of node n at time t
T_n^t	the transmission time between node n and service device
T_n^c	the computing time of data from node n
E_n^t	the energy consumption of transmission between node n and service device
E_n^c	the energy consumption of processing data from node n

the connection relationship between different nodes, and we have

$$\eta_{n,m} = \begin{cases} 1, & \text{if } n \text{ and } m \text{ are connected and adjacent} \\ 0, & \text{otherwise.} \end{cases} \quad (1)$$

$\mathcal{C} = \{\varepsilon_n : n \in \mathcal{N}\}$ denotes the traffic destiny of each node. We define the road traffic complexity of node n at the k-th sampling as:

$$\varepsilon_n(t_k) = s_n^s + s_n^d(t_k), \quad (2)$$

where t_k is the time slot of the k-th sampling. s_n^s is the static complexity. Its value increases with the complexity of the road environment and is constant. $s_n^d(t_k)$ is the dynamic complexity. Its value is positively correlated with the current road vehicle and pedestrian density, which is estimated by cameras of the service device scanning the road.

AoI is a novel metric to assess the freshness of received data [29], which is defined as $a(t) = t - u(t)$, where $u(t)$ is the time of the last update. AoI reflects the decay of data correlation over time. According to traffic complexity and AoI, we propose the weighted AoI. The weighted AoI of node n can be written as

$$a_n(t) = \varepsilon_n(t)(t - u_n(t)), \quad (3)$$

where $u_n(t)$ denotes the latest update time of the road node n. The definition of weighted AoI causes nodes with congested vehicles or pedestrians to have a higher sampling frequency.

We consider that sampling can update other node data, but the updated weighted AoI has a spatial decay trend. Therefore, we define spatial correlation to represent the weighted AoI decay of data sharing for different road nodes. The spatial correlation of adjacent road nodes can be written as $\varphi_{m,n} =$
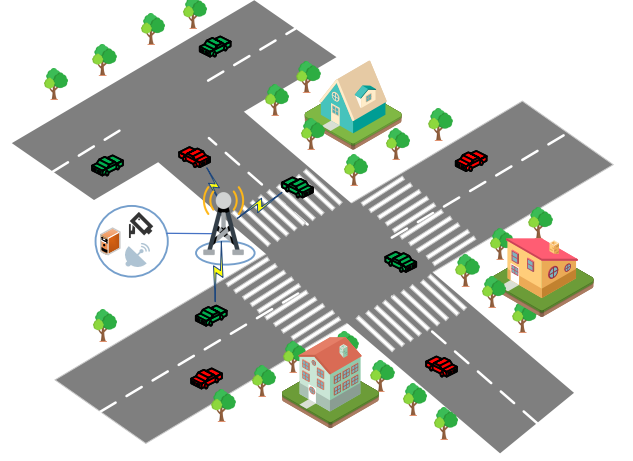

Fig. 1. Service device for traffic management in vehicular network.

$\rho_{m,n}^s d_{m,n}$, where $\rho_{m,n}^s$ and $d_{n,m}$ denotes the coefficient of spatial correlation and the distance between node n and node m respectively [30]. Let $\varphi_{m,n}$ be the path length between adjacent nodes in directed graph $\mathcal{G}(\mathcal{N}, \mathcal{C}, \mathcal{E})$. The service device can obtain the spatial correlation between all nodes by using the Dijkstra algorithm to search for the shortest path. Then, the weighted AoI of node n updated by the sampling data of node m can be expressed as

$$a_n(t) = \tau_t \varepsilon_n(t)(t - u_m(t)) + \tau_s \varphi_{m,n}, \quad (4)$$

where τ_t and τ_s are weight coefficients that give the service device the ability to consider temporal correlation ($\tau_s = 0$), spatial correlation ($\tau_t = 0$), or both.

Figure 3 shows the weighted AoI evolution of node n. Note that the service device collects the data of node n at time $t_{n,k}$ and finishes processing the data at $t'_{n,k}$. Therefore, node n updates weighted AoI at $t'_{n,k}$. Moreover, the service device collects the data of node m at time $t_{m,k}$ and finishes processing the data at $t'_{m,k}$. Accroding to formula (4), The weighted AoI of node n should add spatial correlation variable $\varphi_{m,n}$.

B. Sampling Slot Model

To reduce the weighted AoI of the data, we design a sampling strategy with no-wait transmission and no-wait computing. As shown in Fig. 4, to ensure that the transmission resources and computing resources are sufficient , the sampling time should be after the completion of the previous sample transmission. Besides, the computing device should process the last sampled data before computing device receiving new data. We define samping nodes as a set $\mathcal{M} = \{1, 2, ..., M\}$ ($\mathcal{M} \subseteq \mathcal{N}$). Assuming that the timestamp of k-th sampling is t_k, the transmission time and computing time of k-th sampling in node m are $T_{m,k}^t$ and $T_{m,k}^c$, respectively. t_k should satisfy the following constraints:

$$t_k \geq t_{k-1} + T_{m,k-1}^t + T_{m,k-1}^c - T_{m,k}^t, \quad \forall m \in \mathcal{M}, \quad (5)$$

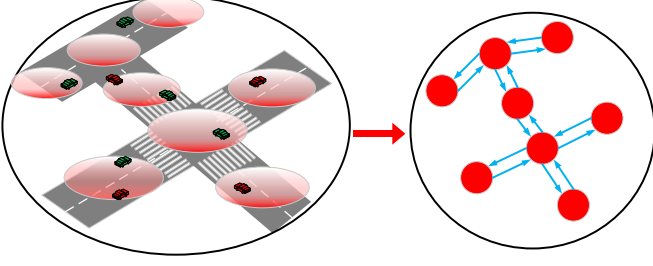$$t_k \geq t_{k-1} + T_{m,k}^t, \quad \forall m \in \mathcal{M}. \quad (6)$$

Fig. 2. Directed Graph Model of Road Segments in IoV.

Fig. 3. Illustration of weighted AoI update.

The sampling timestamp should be as small as possible. According to constraint (5) (6), the sampling timestamp can be written as

$$t_k = \min \left\{ t_{1,k-1} + T_{1,k-1}^t + T_{1,k-1}^c - T_{1,k}^t, t_{1,k-1} + T_{1,k}^t ,\right.$$
$$\left. ..., t_{M,k-1} + T_{M,k-1}^t + T_{M,k-1}^c - T_{M,k}^t , t_{M,k-1} + T_{M,k}^t \right\}. \tag{7}$$

Note that the transmission and computing of each samping slot are independent. Therefore, we discuss sampling decisions and resource allocation models for a single slot.

C. Transmission and Computing Model

We define a binary variable $x_n \in \{0,1\}$ to denote whether to sample node n. We have

$$x_n = \begin{cases} 1, & \text{if sampling node } n \\ 0, & \text{otherwise.} \end{cases} \tag{8}$$

Due to the limitation of sensing ability, the service device needs to cooperate with onboard sensors on the road to collect detailed traffic data. We ignore the samping time of the onboard sensors collect data. We ignore the time the onboard sensors collect data. Assuming that the sampled data size of each node is constant b_n, the total bandwidth dedicated to collecting traffic data is B. The transmission time of the data collected by node n to the service device can be written as

$$T_n^t = \frac{x_n b_n}{\gamma_n B \log(1 + \frac{P_n G_n}{\sigma^2})}, \tag{9}$$

where P_n is the transmit power of sampling vehicle, σ^2 is the background noise, G_n is the channel gain between sampling vehicle and service device, and γ_n is the proportion of bandwidth allocation. γ_n should satisfy the constraint as shown by the following:

$$\sum_{n=1}^{N} x_n \gamma_n \leq 1. \tag{10}$$

Assuming that the CPU cycles required to computing per bit are positive correlation with the traffic complexity. Computing time of traffic data can be written as
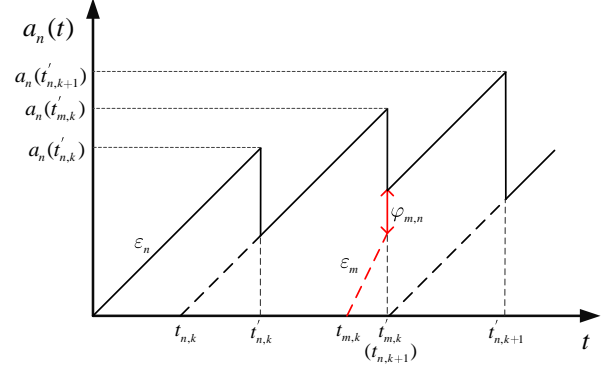
$$T_n^c = \frac{\xi b_n \varepsilon_n}{f_n}, \tag{11}$$

where ξ is the conversion coefficient between computing complexity and traffic complexity. f_n is the computing rate for processing node n, it should meet the constraint as follow:

$$\sum_{n=1}^{N} x_n f_n \leq F_{max}, \tag{12}$$

where F_{max} is the maximum CPU frequency of the computing device. Then, the total execution time of samping node n can be written as

$$T_n^{total} = T_n^t + T_n^c. \tag{13}$$

According to (4), the weighted AoI of node n will be updated to t_n^{total}. The weighted AoI of unsampled nodes can also be updated by sharing data from sampled nodes. It can be written as

$$a_n(t_k) = \min \left\{ \varepsilon_1 T_1^{total} + \varphi_{1,n}, ..., \right.$$
$$\left. \varepsilon_M T_M^{total} + \varphi_{M,n}, a_n(t_{k-1}) \right\}. \tag{14}$$

D. Energy Consumption Model and Weighted AoI Constraint

Motivated by the above discussions, we consider the energy consumption of transmission between vehicle and service device. It can be written as

$$E_n^t = \frac{b_n P_n}{\gamma_n B \log(1 + \frac{P_n G_n}{\sigma^2})}. \tag{15}$$

The computing device applies the dynamic voltage and frequency scaling (DVFS) technique [31]. Assuming that κ is the effective capacitance coefficient, the energy consumption can be written as follows:

$$E_n^c = \kappa(\xi b_n \varepsilon_n) f_n^2. \tag{16}$$

Then, the total energy consumption can be written as

$$E = \sum_{n=1}^{N} x_n \left(E_n^t + E_n^c \right)$$
$$= \sum_{n=1}^{N} x_n \left(\frac{x_n b_n P_n}{\gamma_n B \log(1 + \frac{P_n G_n}{\sigma^2})} + \kappa \xi b_n \varepsilon_n f_n^2 \right). \tag{17}$$
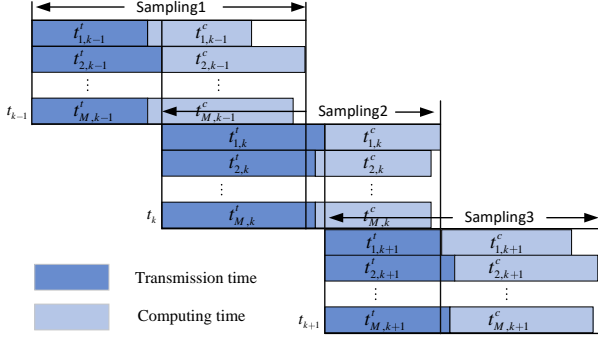
Fig. 4. Sampling slot model without transmission wait and computing wait.

We define a binary variable $z_{m,n}$ to denote whether the weighted AoI of node n is updated by the sampling of node m. We have

$$z_{m,n} = \begin{cases} 1, & \text{if } m = \arg\min\{\varepsilon_1 T_1^{total} + \varphi_{1,n}, ... \\ & , \varepsilon_M T_M^{total} + \varphi_{M,n}, a_n(t_{k-1})\} \\ 0, & \text{otherwise.} \end{cases} \quad (18)$$

In order to ensure the freshness of traffic data, each node needs to satisfy the peak weighted age of information (PWAoI) constraint [32]:

$$z_{m,n}\varepsilon_n(t_k + T_{m,k}^{total} - t_{k-1} - T_{m,k-1}^{total}) + a'_n \leq A'_{max}, \\ \forall n \in \mathcal{N}, \forall m \in \mathcal{M}, \quad (19)$$

where a'_n is the initial weighted AoI of node n for this sampling slot. The left-hand side of constraint is the peak weighted AoI of node n. However, the constraint cannot limit a'_n. High initial weighted AoI will make this constraint of the next sampling slot hard to satisfy. Therefore, we constrain the updated weighted AoI of each node as shown by the following:

$$a_n \leq A_{max}, \forall n \in \mathcal{N}. \quad (20)$$

E. Problem Formulation

This section formulate joint sampling selection and resource allocation as an optimization problem. Our objective is to minimize transmission and computing energy consumption. The design variables include the sampling selection $\{x_n\}$, the proportion of bandwidth allocation $\{\gamma_n\}$ and computing rate allocation $\{f_n\}$. The optimization problem is formulated as

$$P1: \min_{\{x_n, \gamma_n, f_n\}} E$$
$$s.t. \quad (10), (12), (19), (20), \quad (21)$$
$$x_n \in \{0, 1\}, \gamma_n \geq 0, f_n \geq 0. \quad (22)$$

IV. OPTIMAL SAMPING SELECTION AND RESOURCE ALLOCATION

Note that solving P1 is challenging with a non-convex constraint (19) and an integer constraint (22). Therefore, we decouple P1 into sampling selection problem and resource allocation problem.

A. Optimal Sampling Selection Decision

Optimal sampling selection decision is under given $\{\gamma_n, f_n\}$. The problem can be formulated as

$$P1.1: \min_{\{x_n\}} \quad \sum_{n=1}^{N} x_n \left(E_n^t + E_n^c\right)$$
$$s.t. \quad (19), (20), \quad (23)$$
$$x_n \in \{0, 1\}. \quad (24)$$

Problem is a 0-1 integer programming problem. It is still challenging to solve $P1.1$ with complex constraints (19) and (20). Therefore, we first calculate t_n^{total} of each node by given $\{\gamma_n, f_n\}$. According to (14), we define a binary variable set $\mathcal{Y} = \{y_{1,1}, ..., y_{M,N}\}$ to denote whether sampling node m satisfy constraint $\varepsilon_n t_m^{total} + a'_n \leq A'_{max}$ and $a_n \leq A_{max}$ for node n. We have

$$y_{n,m} = \begin{cases} 1, & \text{if } m \text{ satisfy the weighted AoI constraint for } n \\ 0, & \text{otherwise.} \end{cases} \quad (25)$$

The objective of the sampling selection decision is to minimize energy consumption while satisfying weighted AoI constraints for each node. For each sampling node m, there is a set of nodes n satisfying weighted AoI constraints ($y_{n,m} = 1$). P1.1 can be tranform into a minimum set cover problem, and we can further relax x_n. Problem can be formulated as

$$P1.2: \min_{\{x_n\}} \quad \sum_{n=1}^{N} x_n \left(E_n^t + E_n^c\right)$$
$$s.t. \quad \sum_{m=1}^{N} y_{m,n} x_n \geq 1, \quad n \in \mathcal{N}, \quad (26)$$
$$0 \leq x_n \leq 1, \quad n \in \mathcal{N}. \quad (27)$$

Note that P1.2 is a linear programming problem, and we can obtain an optimal fractional solution $\{x_n^{**}\}$ with a linear programming solver. Moreover, we use LP rounding algorithms to get an integer solution of P1.1 as follows:

$$x_n^* = \begin{cases} 1, & \text{if } x_n^{**} \geq 1/N, \\ 0, & \text{otherwise.} \end{cases} \quad (28)$$

B. Optimal Resource Allocation Decision

Resource allocation decision is to obtain optimal solution $\{\gamma_n^*, f_n^*\}$ under optimal sampling selection $\{x_n^*\}$. For given $\{x_n^*\}$, weighted AoI constraints (19) (20) can be transformed into time constraints as follow:

$$z_{m,n} t_{m,k}^{total} \leq \frac{A'_{max} - (a'_n + t_k - t_{k-1} - t_{m,k-1}^{total})}{\varepsilon_n}, \quad (29)$$
$$\forall n \in \mathcal{N}, \forall m \in \mathcal{M}$$

$$z_{m,n} t_{m,k}^{total} \leq \frac{A_{max} - \varphi_{m,n}}{\varepsilon_n}, \forall n \in \mathcal{N}. \quad (30)$$

Then, the optimal problem of resource allocation can be formulated as

$$P1.3: \min_{\{\gamma_m, f_m\}} \quad E$$

$$s.t. \quad \sum_{m=1}^{M} \gamma_m \leq 1, \tag{31}$$

$$\sum_{m=1}^{M} f_m \leq F_{max}, \tag{32}$$

$$t_m^{total} \leq A_m, \forall m \in \mathcal{M}, \tag{33}$$

$$\gamma_m \geq 0, f_m \geq 0. \tag{34}$$

Where $A_m \overset{\Delta}{=} \min\{\frac{A'_{\max} - (a'_1 + t_k - t_{k-1} - t_{m,k-1}^{total})}{z_{m,1}\varepsilon_1}, \frac{A_{\max} - \varphi_{m,1}}{z_{m,1}\varepsilon_1}, ..., \frac{A_{\max} - \varphi_{m,N}}{z_{m,N}\varepsilon_N}\}$, constraint (33) is the combined constraint of (29) and (30).

Lemma 1: $P1.3$ is a convex problem.

Proof: See the Appendix. ∎

The Lagrangian function of $P1.3$ is

$$
\begin{aligned}
\mathcal{L} = & \sum_{m=1}^{M}\left(\kappa\xi b_m\varepsilon_m f_m^2 + \frac{x_m b_m P_m}{\gamma_m B\log(1+\frac{p_m G_m}{\sigma^2})}\right) \\
& + \mu\left(\sum_{m=1}^{M}\gamma_m - 1\right) + \lambda\left(\sum_{m=1}^{M} f_m - F_{max}\right) \\
& + \sum_{m=1}^{M}\theta_m\left(\frac{\kappa\xi b_m\varepsilon_m}{f_m} + \frac{b_m}{\gamma_m B\log(1+\frac{P_m G_m}{\sigma^2})} - A_m\right) \\
& - \sum_{m=1}^{M}\phi_m\gamma_m - \sum_{m=1}^{M}\psi_m f_m.
\end{aligned}
\tag{35}
$$

where μ, λ, θ_m, ϕ_m and ψ_m are the Lagrangian multipliers. Then, we can obtain the dual problem of $P1.3$ as follows:

$$\max_{\{\mu,\lambda,\theta_m\}} \quad \min \mathcal{L}$$

$$
s.t. \quad \mu \geq 0, \ \lambda \geq 0, \tag{36}
$$
$$
\theta_m \geq 0, \ \phi_m \geq 0, \ \psi_m \geq 0, \ \forall m \in \mathcal{M}.
$$

We can solve $P1.3$ using the KKT conditions. Assuming that $\{\mu^*, \lambda^*, \theta_m^*, \phi_m^*, \psi_m^*\}$ is the optimal solution to the Lagrange dual problem of $P1.3$. As $P1.3$ is a convex problem, the following KKT conditions are necessary and sufficient to solve primal and dual optimal problem [33].

$$
\gamma_m^* \geq 0, \ f_m^* \geq 0, \ \mu^* \geq 0, \ \lambda^* \geq 0, \tag{37}
$$
$$
\phi_m^* \geq 0, \ \psi_m^* \geq 0, \ \theta_m^* \geq 0, m \in \mathcal{M},
$$

$$
\sum_{m=1}^{M}\gamma_m^* \leq 1, \ \sum_{m=1}^{M} f_m^* \leq F_{max}, \tag{38}
$$

$$
\frac{\kappa\xi b_m\varepsilon_m}{f_m^*} + \frac{b_m}{\gamma_m^* B\log(1+\frac{P_m G_m}{\sigma^2})} \leq A_m, \ m \in \mathcal{M}, \tag{39}
$$

$$
\mu^*\left(\sum_{m=1}^{M}\gamma_m^* - 1\right) = 0, \lambda^*\left(\sum_{m=1}^{M} f_m^* - F_{mec}\right) = 0, \tag{40}
$$

$$
\theta_m^*\left(\frac{\kappa\xi b_m\varepsilon_m}{f_m^*} + \frac{b_m}{\gamma_m^* B\log(1+\frac{P_m G_m}{\sigma^2})} - A_m\right) = 0, \ m \in \mathcal{M}, \tag{41}
$$

$$
\phi_m^*\gamma_m^* = 0, \ \psi_m^* f_m^* = 0, \ m \in \mathcal{M}, \tag{42}
$$

$$
\begin{aligned}
\frac{\partial\mathcal{L}}{\partial\gamma_m^*} = & \frac{-b_m P_m}{\gamma_m^{*2} B\log(1+\frac{P_m G_m}{\sigma^2})} + \mu^* - \phi_m^* \\
& - \frac{\theta_m^* b_m}{\gamma_m^{*2} B\log(1+\frac{P_m G_m}{\sigma^2})} = 0, \ m \in \mathcal{M},
\end{aligned}
\tag{43}
$$

$$
\frac{\partial\mathcal{L}}{\partial f_m^*} = 2\kappa\xi b_m\varepsilon_m f_m^* + \lambda^* - \psi_m^* - \frac{\theta_m^*\xi b_m\varepsilon_m}{f_m^{*2}} = 0, \ m \in \mathcal{M}. \tag{44}
$$

Where (37), (38), (39) and (40) are the primal and dual constraints, (41) and (42) denotes the complementary slackness conditions, and (43) and (44) denote the necessary conditions for $\gamma_m = \gamma_m^*$, $f_m = f_m^*$, $m \in \mathcal{M}$, respectively. To start with, we establish the following lemma on the optimal solutions.

Lemma 2: For the optimal solution ϕ_m^* and ψ_m^*, they must be hold that $\phi_m^* = \psi_m^* = 0$.

Proof: We prove Lemma 2 by contradiction. We suppose that $\phi_m^* \neq 0$. Based on the constraint (42), it must hold that $\gamma_m^* = 0$. For the constraint (39), $\frac{\xi b_m\varepsilon_m}{f_m^*} + \frac{b_m}{\gamma_m^* B\log(1+\frac{P_m G_m}{\sigma^2})} = +\infty$. Accordingly, γ_m^* can not satisfy the constraint. Similarly, we suppose that $\psi_m^* \neq 0$. Based on the constraint (42), it must hold that $f_m^* = 0$. For the constraint (39), $\frac{\xi b_m\varepsilon_m}{f_m^*} + \frac{b_m}{\gamma_m^* B\log(1+\frac{P_m G_m}{\sigma^2})} = +\infty$. f_m^* can not satisfy the constraint. Therefore, the optimal solution ϕ_m^* and ψ_m^* must be hold that $\phi_m^* = \psi_m^* = 0$. ∎

Lemma 3: For the optimal solution μ^*, it must be hold that $\mu^* \neq 0$.

Proof: We prove Lemma 3 by contradiction. We suppose that $\mu^* = 0$, the constraint (43) can be written as $\frac{-b_m P_m}{\gamma_m^{*2} B\log(1+\frac{P_m G_m}{\sigma^2})} - \frac{\theta_m^* b_m}{\gamma_m^{*2} B\log(1+\frac{P_m G_m}{\sigma^2})} = 0$, $m \in \mathcal{M}$. Obviously, $\frac{-b_m P_m}{\gamma_m^{*2} B\log(1+\frac{P_m G_m}{\sigma^2})} - \frac{\theta_m^* b_m}{\gamma_m^{*2} B\log(1+\frac{P_m G_m}{\sigma^2})} < 0$. Therefore, $\mu^* \neq 0$. ∎

To obtain $\{\mu^*, \lambda^*, \theta_m^*\}$, we consider four cases: i) if the KKT conditions are satisfied when $\lambda^* = 0$, $\theta_m^* = 0$. We set $\lambda^* = 0$, $\theta_m^* = 0$, and start a bisection search for μ until the constraint (38). (ii) if the KKT conditions are satisfied when $\theta_m^* = 0$. Similarly, we set $\theta_m^* = 0$, and start a bisection search for μ^* and λ^* until the constraint (38). (iii) if the KKT conditions are satisfied when $\lambda^* = 0$. We set $\lambda^* = 0$, and start a two-layer bisection search for μ and θ_m until constraint (38) and (39). (iv) if $\lambda^* \neq 0$ and $\theta_m^* \neq 0$, we can start a two-layer bisection search for μ^*, λ^* and θ_m^* until constraint (38) and (39). The two-layer biosection search algorithm is described in Algorithm 1.

C. Joint Sampling Selection and Resource Allocation Algorithm

In this section, a joint sampling selection and resource allocation algorithm (JSRA) is proposed to solve problem $P1$. JSRA is shown in Algorithm 2. To be specific, we decouple

Algorithm 1 Two-Layer Bisection Search for μ, λ and θ_m

1: initialize all $\theta_m^{min} = 0$, θ_m^{max}, $m \in \mathcal{M}$;
2: **while** $\exists m \in \mathcal{M}$, $\theta_m^{\max} - \theta_m^{\min} > \kappa_1$ **do**
3:    **for** $m = 1 : M$ **do**
4:       setting $\theta_m = \frac{\theta_m^{\max} + \theta_m^{\min}}{2}$;
5:    **end for**
6:    initialize $\mu^{\min} = 0$, $\mu^{\max}$;
7:    **while** $\mu^{\max} - \mu^{\min} > \kappa_2$ **do**
8:       $\mu = \frac{\mu^{\max} + \mu^{\min}}{2}$;
9:       calculate γ_m according to (43);
10:       **if** $\sum_{m=1}^{M} \gamma_m^* \leq 1$ **then**
11:         $\mu^{max} = \mu$;
12:       **else**
13:         $\mu^{min} = \mu$;
14:       **end if**
15:    **end while**
16:    **while** $\lambda^{\max} - \lambda^{\min} > \kappa_3$ **do**
17:       $\lambda = \frac{\lambda^{\max} + \lambda^{\min}}{2}$;
18:       calculate f_m according to (44);
19:       **if** $\sum_{m=1}^{M} f_m^* \leq F_{mec}$ **then**
20:         $\lambda^{\max} = \lambda$;
21:       **else**
22:         $\lambda^{\min} = \lambda$;
23:       **end if**
24:    **end while**
25:    **for** $m = 1 : M$ **do**
26:       **if** $\frac{\xi b_m \varepsilon_m}{f_m^*} + \frac{b_m}{\gamma_m^* B \log(1 + \frac{P_m G_m}{\sigma^2})} \leq A_m$ **then**
27:         $\theta_m^{\max} = \theta_m$;
28:       **else**
29:         $\theta_m^{\min} = \theta_m$;
30:       **end if**
31:    **end for**
32: **end while**

Algorithm 2 Two-Layer Bisection Search for μ, λ and θ_m

1: initialize all $\gamma_n^* = 1, f_n^* = F_{\max}, n \in \mathcal{N}$;
2: **repeat**
3:    Based on γ_n^* and f_n^*, calculate t_m^{total} according to (9)(11)(13);
4:    **for** $y_{m,n} \in \mathcal{Y}$ **do**
5:       **if** $\varepsilon_n t_m^{total} + a_n' \leq A_{\max}'$ and $a_n \leq A_{\max}$ **then**
6:         Set $y_{m,n} \leftarrow 1$;
7:       **else**
8:         Set $y_{m,n} \leftarrow 0$;
9:       **end if**
10:    **end for**
11:    Solve problem $P1.2$ to obtain x_n^{**} by LP solver;
12:    **if** $x_n^{**} \geq 1/N$ **then**
13:       $x^* = 1$;
14:    **else**
15:       $x^* = 0$;
16:    **end if**
17:    Based on x_n^*, obtain Lagrange multipliers μ, λ and θ_m by Algorithm 1;
18:    **for** $n \in \mathcal{M}$ **do**
19:       Calculate γ_n^* and f_n^* according to (43)(44);
20:    **end for**
21: **until** Convergence

the number of iterations is K. Therefore, the computational complexity of JSRA is $\mathcal{O}(KMN + KN^{3.5}\log_2(1/\rho) + KM\log_2(\theta_m^{\max}/\kappa_1)\log_2(\lambda^{\max}\mu^{\max}/\kappa_2\kappa_3))$.

Next, we analyze the convergence of JSRA in the following theorem. A similar approach is applied to prove the convergence in [34].

Theorem 1: The algorithm JSRA is always converges.

Proof: The proof is established by showing that the energy consumption (17) is noinreasing when the set of design variables $\{(x_n, \gamma_n, f_n)|n \in \mathcal{N}\}$ is updated. Assuming that $E_{al}^{(t)}$ is the energy consumption for t iterations of algorithm, we have

$$
\begin{aligned}
E_{al}^{(t-1)} &= E(\{(x_n^{(t-1)}, \gamma_n^{(t-1)}, f_n^{(t-1)})|n \in \mathcal{N}\}) \\
&\overset{(a)}{\geq} E(\{(x_n^*(\{\gamma_n^{(t-1)}, f_n^{(t-1)})|n \in \mathcal{N}\}), \\
&\quad \gamma_n^{(t-1)}, f_n^{(t-1)})|n \in \mathcal{N}\}) \\
&= E(\{(x_n^{(t)}, \gamma_n^{(t-1)}, f_n^{(t-1)})|n \in \mathcal{N}\}) \qquad (45) \\
&\overset{(b)}{\geq} E(\{(x_n^{(t)}, \gamma_n^*(\{x_n^{(t)}|n \in \mathcal{N}\}), \\
&\quad f_n^*(\{x_n^{(t)}|n \in \mathcal{N}\}))|n \in \mathcal{N}\} \\
&= E(\{(x_n^{(t)}, \gamma_n^{(t)}, f_n^{(t)})|n \in \mathcal{N}\}) = E_{al}^{(t)}
\end{aligned}
$$

where $x_n^*(\{\gamma_n^{(t-1)}, f_n^{(t-1)})|n \in \mathcal{N}\})$ denotes the optimal sampling selection under $\gamma_n^{(t-1)}$ and $f_n^{(t-1)}$, $\gamma_n^*(\{x_n^{(t)}|n \in \mathcal{N}\})$ and $f_n^*(\{x_n^{(t)}|n \in \mathcal{N}\})$ denote the optimal bandwidth allocation and computing rate allocation under $x_n^{(t)}$ respectively. Inequality (a) is due to $x_n^*(\{\gamma_n^{(t-1)}, f_n^{(t-1)})|n \in \mathcal{N}\})$ is the

$P1$ into node selection ($P1.1$) and resource allocation ($P1.3$). First, we initialize the resource allocation of all nodes to a large value regardless of resource constraints. Then we solve $P1$ by alternately optimizing $P1.1$ and $P1.3$. The algorithm repeats the process of alternating optimization until convergence.

D. Algorithm complexity and convergence analysis

This section will analyze the computational complexity of JSRA (Algorithm 2). At each iteration of JSRA, the computational complexity of obtaining $y_{m,n}$ (line 4-10) is $\mathcal{O}(MN)$. Assuming that we solve $P1.2$ by interior point method, and solution accuracy is ρ. The complexity of solving $P1.2$ (line 11) is $\mathcal{O}(N^{3.5}\log_2(1/\rho))$.

For Two-Layer Bisection Search (Algorithm 1), the computational complexity of the second layer of Bisection Search is $\mathcal{O}(\log_2(\mu^{\max}/\kappa_2))$ and $\mathcal{O}(\log_2(\lambda^{\max}/\kappa_3))$ respectively. The complexity of Algorithm 1 (line 17) is $\mathcal{O}(M\log_2(\theta_m^{\max}/\kappa_1)(\log_2(\lambda^{\max}/\kappa_3) + \log_2(\mu^{\max}/\kappa_2))) = \mathcal{O}(M\log_2(\theta_m^{\max}/\kappa_1)\log_2(\lambda^{\max}\mu^{\max}/\kappa_2\kappa_3))$. Assuming that

optimal solution of $P1.1$ and its corresponding energy consumption is the minimum under $\gamma_n^{(t-1)}$ and $f_n^{(t-1)}$. Inequality (b) is due to $\gamma_n^*(\left\{x_n^{(t)}|n \in \mathcal{N}\right\})$ and $f_n^*(\left\{x_n^{(t)}|n \in \mathcal{N}\right\})$ are optimal solutions of $P1.3$ and the corresponding energy consumption is the minimum under $x_n^{(t)}$. Therefore, the energy is nonincreasing after the update of sampling selection, bandwidth allocation and computing rate allocation.

Obviously, the total energy consumption is always positive according to formula (17) during each iteration. Since the energy consumption is nonincreasing in each iteration according to (45) and the energy consumption is finitely low-bounded by zero, algorithm JSRA must be converge. ∎

V. NUMERICAL RESULTS

We conduct extensive experiments with vehicle trajectories simulated by Simulation of Urban Mobility (SUMO). And the simulation results are provided to evaluate the performance of proposed method.

A. Simulation of Urban Mobility (SUMO) and parameters setting

TABLE II
TABLE OF SIMULATION PARAMETER SETTINGS

Parameter	Value
Bandwidth: B	4MHz [25]
Transmission power of vehicles: P_n	1W [36]
Background noise: ω_0	-100dBm [37]
Effective capacitance coefficient : κ	10^{-28} [38]
The maximum computing capacity: F_{max}	5G cycles/s
input data size: b_n	$0.1 \sim 1$Mbit [39]
conversion coefficient: ξ	10
length of road segment	$50 \sim 150$m
number of nodes	26

SUMO is an simulation tool designed to handle vehicualr networks [35]. We extract a $500{\times}500$ m^2 area from OpenStreetMap, which is shown in Figure 5. We use OSM tools

to generate different densities of vehicle flow and pedestrians. Vehicles are randomly generated at the simulation boundary and deleted when driving out of the boundary. Besides, we generate directed graphs according to the connections between road segments. Assume that the simulation scenario is within the coverage of an RSU. The main parameters used in the simulations are summarized in Table 1.

B. Impact of different maximum PWAoI constraints

To evaluate the impact of PWAoI constraint, we compare the energy consumption and AoI violation probability [24] under different maximum PWAoI constraints. PWAoI violations are mainly due to limited resources unable to execute huge computing tasks. We show numerical results in Fig. 6 and Fig. 7. Obviously, Lowering maximum PWAoI increase the energy consumption and PWAoI violation probability. Note that when vehicles are dense (number of vehicles > 80), the PWAoI violation probability is high. This is because the resource usage is approaching saturation, and the slowing down of the slope of the "maximum PWAoI = 0.1" curve in Fig. 6 can also reflect this phenomenon.
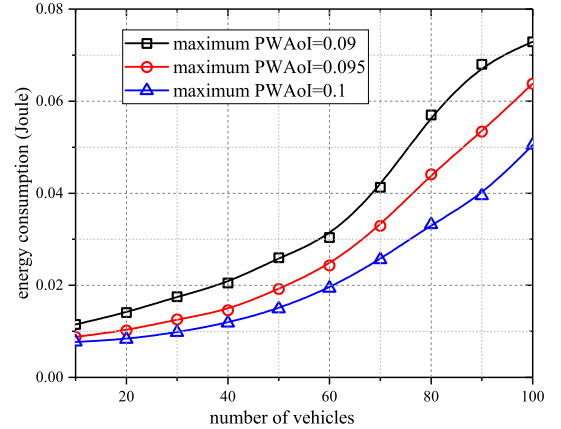

Fig. 6. Energy consumption vs. number of vehicles under different maximum PWAoI constraints.

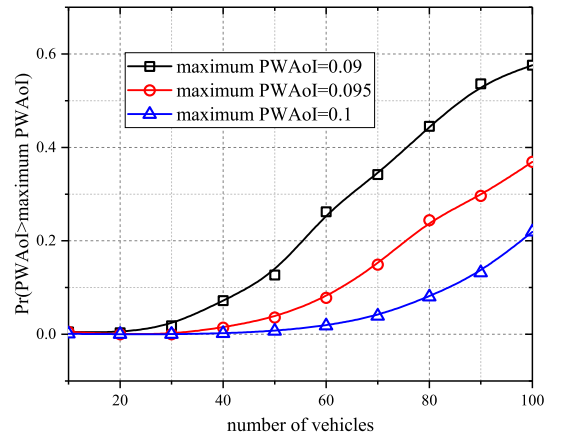Fig. 5. Scenario considered during the experiments.

Fig. 7. PWAoI violation probability vs. number of vehicles under different maximum PWAoI constraints.
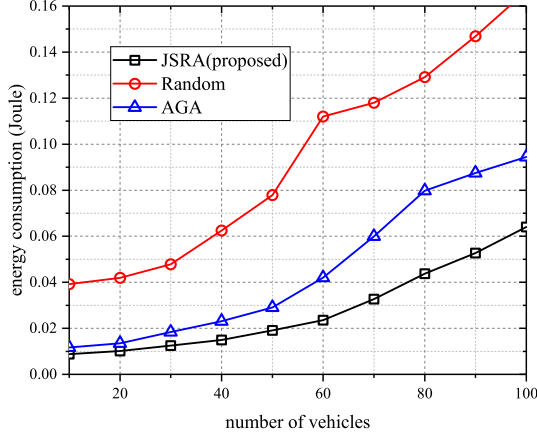
Fig. 8. Comparison of energy consumption under different schemes with maximum PWAoI=0.09.
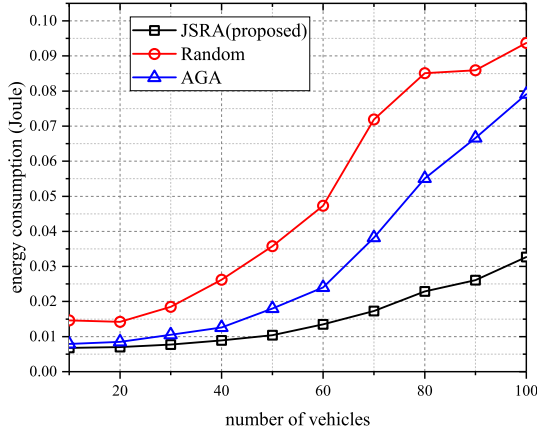

Fig. 9. Comparison of energy consumption under different schemes with maximum PWAoI=0.12.
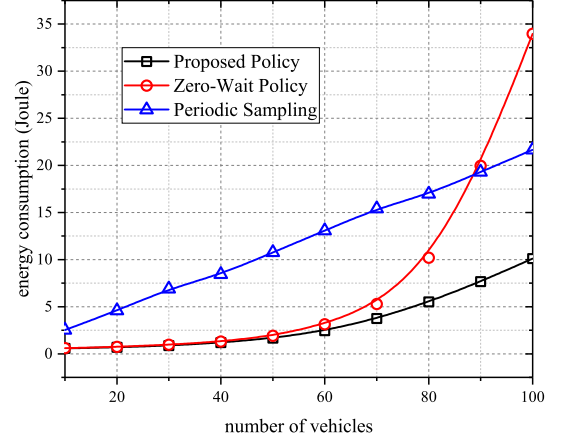

Fig. 10. Comparison of energy consumption under different sampling strategies with maximum PWAoI=0.09.

Fig. 11. Comparison of energy consumption under different sampling strategies with maximum PWAoI=0.12.

C. Performance Comparison for JSRA

In our scenario, the policy must satisfy the AoI constraint. To verify the performance of JSRA, we choose the following benchmark schemes.

1) AoI-Based Greedy Algorithm (AGA) Node Selection: The RSU greedily selects sampling nodes in the node-set with the most significant number of nodes that satisfy constraints according to the PWAoI [40], and repeats this step for selection among the remaining nodes that do not satisfy the constraints.

2) Random Node Selection: The RSU randomly selects sampling nodes in the node-set with the most significant number of nodes that satisfy constraints, and repeats this step for selecting the remaining nodes that do not satisfy constraints. Fig. 8 and Fig. 9 show the energy consumption versus the number of vehicles, where maximum PWAoI is 0.09ms and 0.12ms respectively. Evidently, the performance of the proposed JSRA significantly outperforms Random and AGA in different PWAoI constraints. The number of sampling nodes selection is a crucial factor affecting energy consumption. Compared with other schemes, the Random strategy may select additional sampling nodes, resulting in data redundancy and increased energy consumption. Note that the energy consumption curve of Random scheme will show
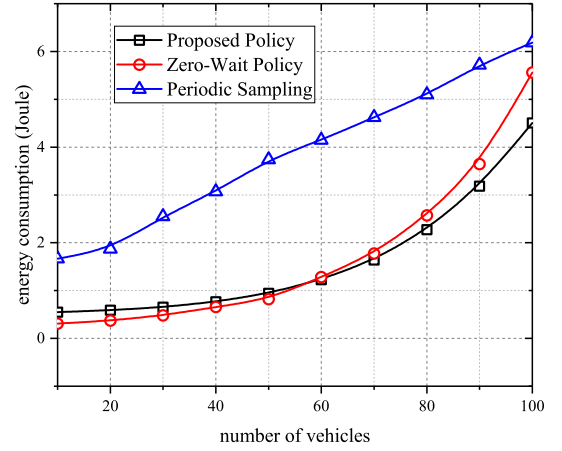
a different trend from a certain point. The reason is that the service device need to sample more nodes with the number of vehicles to meet the PWAoI constraints. The AGA strategy presents similar numerical results under different maximum PWAoI constraints. The reason is that AGA is an age-aware strategy, which preferentially selects nodes with lower AoI. So, it is easier to satisfy strict constraints without allocating excessive resources.

D. Performance Comparison for proposed sampling strategy

Next, we compare the proposed sampling policy concerning two benchmark policies named zero-wait and periodic sampling.

1) Zero-Wait Policy: Zero-Wait policy minimizes the peak age by eliminating the waiting time [41]. RSU collects new data after the previous data collection, transmission and computation.

2) Periodic Sampling: RSU periodically collects data from each node at a set frequency. Collection period is set according to PWAoI constraints.

In the set time slot of the same length, we compare policies to keep PWAoI less than the constrained energy consumption.

Considering the impact of PWAoI constraints on the results, we assume that the zero-wait and periodic sampling strategies have sufficient communication and computing resources. As shown in Fig. 10 and Fig. 11, The zero-wait policy is slightly better than proposed policy in some cases (number of vehicles < 60, where maximum PWAoI $= 0.12$). The reason is that zero-wait policy needs to wait for the last complete sampling process to end before the next sampling. Compared with the proposed policy, it has a lower sampling frequency and is suitable for scenarios with low vehicle density and high maximum PWAoI. However, when the vehicle density increases or the PWAoI constraints are more stringent, the zero-wait method requires more resources to reduce processing latency. The proposed policy can maximize the utilization of resources while reducing the updated AoI so that the data collection and computation generate only a tiny amount of energy consumption. Therefore, the proposed policy exhibits better performance than zero-wait policy and periodic sampling.

VI. Conclusion

In this paper, we have studied the energy minimization problem in vehicular networks, considering AoI constraints. We have modeled the correlation of road segments as a directed graph, and evalute the freshness of data by weighted AoI. A novel sampling slot model has been adopted to reduce AoI. Then, we designed a energy-efficient data collection and resource allocation strategy. Subsequently, we have formulated a energy minimization problem subject to the peak weighted AoI constraints and proposed a JSRA algorithm to obtain the approximate solution. Numerical result based on SUMO demonstrated that the proposed strategy and JSRA alogrithm outperform the existing shcemes. Futhermore, our method shows better performance in scenario with high destiny of pederstrians and vehicles.

Appendix
Proof of Lemma 1

First, we check the convexity of objective fuction. The objective function of the problem ($P1.3$) can be expressed as

$$\min_{\{\gamma_m, f_m\}} f_1(\gamma_m) + f_2(f_m). \tag{46}$$

The second-order derivative of $f_1(\gamma_m)$ with respect to γ_m is

$$\frac{\partial^2 f_1(\gamma_m)}{\partial \gamma_m^2} = \frac{2b_m P_m}{\gamma_m^3 B \log(1 + \frac{P_m G_m}{\sigma^2})}. \tag{47}$$

As $b_m > 0$, $P_m > 0$, $G_m > 0$, $B > 0$ and $\gamma_m > 0$, we have $\frac{\partial^2 f_1(\gamma_m)}{\partial \gamma_m^2} > 0$. The second-order derivative of $f_2(\gamma_m)$ is

$$\frac{\partial^2 f_2(f_m)}{\partial f_m^2} = 2\kappa\xi b_m \varepsilon_m. \tag{48}$$

As $\kappa > 0$, $\xi > 0$ and $\varepsilon_m > 0$, we have $\frac{\partial^2 f_2(f_m)}{\partial f_m^2} > 0$. Therefore, $f_1(\gamma_m)$ and $f_2(f_m)$ are convex function. Due to the convexity preservation of additive operation, the objective function is convex. Evidently, the constraints (31), (32) and (34) are linear convex. Then, we check the convexity of constraint (33).

The constraint (33) can be expressed as

$$g_1(\gamma_m) + g_2(f_m) - A_m \le 0. \tag{49}$$

The second-order derivative of $g_1(\gamma_m)$ is

$$\frac{\partial^2 g_1(\gamma_m)}{\partial \gamma_m^2} = \frac{2b_m}{\gamma_m^3 B \log(1 + \frac{P_m G_m}{\sigma^2})} > 0. \tag{50}$$

And the second-order derivative of $g_2(f_m)$ is

$$\frac{\partial^2 g_2(f_m)}{\partial f_m^2} = \frac{2b_m \varepsilon_m}{f_m^3}. \tag{51}$$

As $f_m > 0$, $\frac{\partial^2 g_2(f_m)}{\partial f_m^2} > 0$. $g_1(\gamma_m)$ and $g_2(f_m)$ are convex functions. Due to the convexity preservation of additive operation, constraint (33) is convex. Therefore, the problem ($P1.3$) is a convex problem.

References

[1] C. Neff, M. Mendieta, S. Mohan, M. Baharani, S. Rogers, and H. Tabkhi, "Revamp2t: Real-time edge video analytics for multicamera privacy-aware pedestrian tracking," *IEEE Internet of Things Journal*, vol. 7, no. 4, pp. 2591–2602, 2020.
[2] Y. Liu, J. Liu, A. Argyriou, L. Wang, and Z. Xu, "Rendering-aware vr video caching over multi-cell mec networks," *IEEE Transactions on Vehicular Technology*, vol. 70, no. 3, pp. 2728–2742, 2021.
[3] L. Zhao, G. Han, Z. Li, and L. Shu, "Intelligent digital twin-based software-defined vehicular networks," *IEEE Network*, vol. 34, no. 5, pp. 178–184, 2020.
[4] S. Aoki, C.-W. Lin, and R. Rajkumar, "Human-robot cooperation for autonomous vehicles and human drivers: Challenges and solutions," *IEEE Communications Magazine*, vol. 59, no. 8, pp. 35–41, 2021.
[5] J. Wang, C. Jiang, K. Zhang, T. Q. S. Quek, Y. Ren, and L. Hanzo, "Vehicular sensing networks in a smart city: Principles, technologies and applications," *IEEE Wireless Communications*, vol. 25, no. 1, pp. 122–132, 2018.
[6] L. Liu, L. Wang, Z. Lu, Y. Liu, W. Jing, and X. Wen, "Cost-and-quality aware data collection for edge-assisted vehicular crowdsensing," *IEEE Transactions on Vehicular Technology*, vol. 71, no. 5, pp. 5371–5386, 2022.
[7] S. Kaul, M. Gruteser, V. Rai, and J. Kenney, "Minimizing age of information in vehicular networks," in *2011 8th Annual IEEE Communications Society Conference on Sensor, Mesh and Ad Hoc Communications and Networks*, 2011, pp. 350–358.
[8] A. M. Bedewy, Y. Sun, and N. B. Shroff, "Minimizing the age of information through queues," *IEEE Transactions on Information Theory*, vol. 65, no. 8, pp. 5215–5232, 2019.
[9] P. Zou, O. Ozel, and S. Subramaniam, "Waiting before serving: A companion to packet management in status update systems," *IEEE Transactions on Information Theory*, vol. 66, no. 6, pp. 3864–3877, 2020.
[10] X. Wu, J. Yang, and J. Wu, "Optimal status update for age of information minimization with an energy harvesting source," *IEEE Transactions on Green Communications and Networking*, vol. 2, no. 1, pp. 193–204, 2018.
[11] J. Wang, K. Zhu, and E. Hossain, "Green internet of vehicles (iov) in the 6g era: Toward sustainable vehicular communications and networking," *IEEE Transactions on Green Communications and Networking*, vol. 6, no. 1, pp. 391–423, 2022.
[12] C. Zheng, D. Feng, S. Zhang, X.-G. Xia, G. Qian, and G. Y. Li, "Energy efficient v2x-enabled communications in cellular networks," *IEEE Transactions on Vehicular Technology*, vol. 68, no. 1, pp. 554–564, 2019.
[13] P. Dong, Z. Ning, R. Ma, X. Wang, X. Hu, and B. Hu, "Noma-based energy-efficient task scheduling in vehicular edge computing networks: A self-imitation learning-based approach," *China Communications*, vol. 17, no. 11, pp. 1–11, 2020.
[14] Z. Li, L. Xiang, and X. Ge, "Age of information modeling and optimization for fast information dissemination in vehicular social networks," *IEEE Transactions on Vehicular Technology*, vol. 71, no. 5, pp. 5445–5459, 2022.

[15] X. Chen, C. Wu, T. Chen, H. Zhang, Z. Liu, Y. Zhang, and M. Bennis, "Age of information aware radio resource management in vehicular networks: A proactive deep reinforcement learning perspective," *IEEE Transactions on Wireless Communications*, vol. 19, no. 4, pp. 2268–2281, 2020.

[16] X. Qin, Y. Xia, H. Li, Z. Feng, and P. Zhang, "Distributed data collection in age-aware vehicular participatory sensing networks," *IEEE Internet of Things Journal*, vol. 8, no. 19, pp. 14 501–14 513, 2021.

[17] S. Zhang, J. Li, H. Luo, J. Gao, L. Zhao, and X. Sherman Shen, "Low-latency and fresh content provision in information-centric vehicular networks," *IEEE Transactions on Mobile Computing*, vol. 21, no. 5, pp. 1723–1738, 2022.

[18] C. Chen, L. Chen, L. Liu, S. He, X. Yuan, D. Lan, and Z. Chen, "Delay-optimized v2v-based computation offloading in urban vehicular edge computing and networks," *IEEE Access*, vol. 8, pp. 18 863–18 873, 2020.

[19] Y. Ni, L. Cai, and Y. Bo, "Vehicular beacon broadcast scheduling based on age of information (aoi)," *China Communications*, vol. 15, no. 7, pp. 67–76, 2018.

[20] M. Chen, Y. Xiao, Q. Li, and K.-c. Chen, "Minimizing age-of-information for fog computing-supported vehicular networks with deep q-learning," in *ICC 2020 - 2020 IEEE International Conference on Communications (ICC)*, 2020, pp. 1–6.

[21] L. Hu, Z. Chen, Y. Dong, Y. Jia, M. Wang, L. Liang, and C. Chen, "Optimal status update in iot systems: An age of information violation probability perspective," in *2020 IEEE 92nd Vehicular Technology Conference (VTC2020-Fall)*, 2020, pp. 1–5.

[22] R. Devassy, G. Durisi, G. C. Ferrante, O. Simeone, and E. Uysal-Biyikoglu, "Delay and peak-age violation probability in short-packet transmissions," in *2018 IEEE International Symposium on Information Theory (ISIT)*, 2018, pp. 2471–2475.

[23] L. Hu, Z. Chen, Y. Dong, Y. Jia, L. Liang, and M. Wang, "Status update in iot networks: Age-of-information violation probability and optimal update rate," *IEEE Internet of Things Journal*, vol. 8, no. 14, pp. 11 329–11 344, 2021.

[24] M. K. Abdel-Aziz, S. Samarakoon, C.-F. Liu, M. Bennis, and W. Saad, "Optimized age of information tail for ultra-reliable low-latency communications in vehicular networks," *IEEE Transactions on Communications*, vol. 68, no. 3, pp. 1911–1924, 2020.

[25] H. Ke, J. Wang, L. Deng, Y. Ge, and H. Wang, "Deep reinforcement learning-based adaptive computation offloading for mec in heterogeneous vehicular networks," *IEEE Transactions on Vehicular Technology*, vol. 69, no. 7, pp. 7916–7929, 2020.

[26] R. Yadav, W. Zhang, O. Kaiwartya, H. Song, and S. Yu, "Energy-latency tradeoff for dynamic computation offloading in vehicular fog computing," *IEEE Transactions on Vehicular Technology*, vol. 69, no. 12, pp. 14 198–14 211, 2020.

[27] W. Zhan, C. Luo, J. Wang, C. Wang, G. Min, H. Duan, and Q. Zhu, "Deep-reinforcement-learning-based offloading scheduling for vehicular edge computing," *IEEE Internet of Things Journal*, vol. 7, no. 6, pp. 5449–5465, 2020.

[28] B. Shang, L. Liu, and Z. Tian, "Deep learning-assisted energy-efficient task offloading in vehicular edge computing systems," *IEEE Transactions on Vehicular Technology*, vol. 70, no. 9, pp. 9619–9624, 2021.

[29] S. Kaul, R. Yates, and M. Gruteser, "Real-time status: How often should one update?" in *2012 Proceedings IEEE INFOCOM*, 2012, pp. 2731–2735.

[30] A. A. Al-Habob, O. A. Dobre, and H. V. Poor, "Age- and correlation-aware information gathering," *IEEE Wireless Communications Letters*, vol. 11, no. 2, pp. 273–277, 2022.

[31] J. M. Kim, Y. G. Kim, and S. W. Chung, "Stabilizing cpu frequency and voltage for temperature-aware dvfs in mobile devices," *IEEE Transactions on Computers*, vol. 64, no. 1, pp. 286–292, 2015.

[32] C. Xu, H. H. Yang, X. Wang, and T. Q. S. Quek, "Optimizing information freshness in computing-enabled iot networks," *IEEE Internet of Things Journal*, vol. 7, no. 2, pp. 971–985, 2020.

[33] S. Boyd, S. P. Boyd, and L. Vandenberghe, *Convex optimization*. Cambridge university press, 2004.

[34] Z. Yang, C. Pan, K. Wang, and M. Shikh-Bahaei, "Energy efficient resource allocation in uav-enabled mobile edge computing networks," *IEEE Transactions on Wireless Communications*, vol. 18, no. 9, pp. 4576–4589, 2019.

[35] D. Krajzewicz, J. Erdmann, M. Behrisch, and L. Bieker, "Recent development and applications of sumo-simulation of urban mobility," *International journal on advances in systems and measurements*, vol. 5, no. 3&4, 2012.

[36] C. Yang, W. Lou, Y. Liu, and S. Xie, "Resource allocation for edge computing-based vehicle platoon on freeway: A contract-optimization approach," *IEEE Transactions on Vehicular Technology*, vol. 69, no. 12, pp. 15 988–16 000, 2020.

[37] Y. Han, E. Ekici, H. Kremo, and O. Altintas, "Resource allocation algorithms supporting coexistence of cognitive vehicular and ieee 802.22 networks," *IEEE Transactions on Wireless Communications*, vol. 16, no. 2, pp. 1066–1079, 2017.

[38] F. Fang, Y. Xu, Z. Ding, C. Shen, M. Peng, and G. K. Karagiannidis, "Optimal resource allocation for delay minimization in noma-mec networks," *IEEE Transactions on Communications*, vol. 68, no. 12, pp. 7867–7881, 2020.

[39] J. Du, F. R. Yu, X. Chu, J. Feng, and G. Lu, "Computation offloading and resource allocation in vehicular networks based on dual-side cost minimization," *IEEE Transactions on Vehicular Technology*, vol. 68, no. 2, pp. 1079–1092, 2019.

[40] Y. Shao, Q. Cao, S. C. Liew, and H. Chen, "Partially observable minimum-age scheduling: The greedy policy," *IEEE Transactions on Communications*, vol. 70, no. 1, pp. 404–418, 2022.

[41] Y. Sun, E. Uysal-Biyikoglu, R. D. Yates, C. E. Koksal, and N. B. Shroff, "Update or wait: How to keep your data fresh," *IEEE Transactions on Information Theory*, vol. 63, no. 11, pp. 7492–7508, 2017.